Hindawi Publishing Corporation
Advances in High Energy Physics
Volume 2013, Article ID 708680, 18 pages
http://dx.doi.org/10.1155/2013/708680

Review Article

Ultrahigh Energy Neutrinos at the Pierre Auger Observatory

P. Abreu,[1] M. Aglietta,[2] M. Ahlers,[3] E. J. Ahn,[4] I. F. M. Albuquerque,[5] D. Allard,[6] I. Allekotte,[7] J. Allen,[8] P. Allison,[9] A. Almela,[10,11] J. Alvarez Castillo,[12] J. Alvarez-Muñiz,[13] R. Alves Batista,[14] M. Ambrosio,[15] A. Aminaei,[16] L. Anchordoqui,[17] S. Andringa,[1] T. Antičić,[18] C. Aramo,[15] E. Arganda,[19,20] F. Arqueros,[20] H. Asorey,[7] P. Assis,[1] J. Aublin,[21] M. Ave,[22] M. Avenier,[23] G. Avila,[24] T. Bäcker,[25] A. M. Badescu,[26] M. Balzer,[27] K. B. Barber,[28] A. F. Barbosa,[29] R. Bardenet,[30] S. L. C. Barroso,[31] B. Baughman,[9,32] J. Bäuml,[33] J. J. Beatty,[9] B. R. Becker,[34] K. H. Becker,[35] A. Bellétoile,[36] J. A. Bellido,[28] S. BenZvi,[3] C. Berat,[23] X. Bertou,[7] P. L. Biermann,[37] P. Billoir,[21] F. Blanco,[20] M. Blanco,[21,38] C. Bleve,[35] H. Blümer,[22,33] M. Boháčová,[39] D. Boncioli,[40] C. Bonifazi,[21,41] R. Bonino,[2] N. Borodai,[42] J. Brack,[43] I. Brancus,[44] P. Brogueira,[1] W. C. Brown,[45] R. Bruijn,[46,47] P. Buchholz,[25] A. Bueno,[48] R. E. Burton,[49] K. S. Caballero-Mora,[50] B. Caccianiga,[51] L. Caramete,[37] R. Caruso,[52] A. Castellina,[2] O. Catalano,[53] G. Cataldi,[54] L. Cazon,[1] R. Cester,[55] J. Chauvin,[23] S. H. Cheng,[50] A. Chiavassa,[2] J. A. Chinellato,[14] J. Chirinos Diaz,[56] J. Chudoba,[39] M. Cilmo,[15] R. W. Clay,[28] M. R. Coluccia,[54] R. Conceição,[1] F. Contreras,[57] H. Cook,[46] M. J. Cooper,[28] J. Coppens,[16,58] A. Cordier,[30] S. Coutu,[50] C. E. Covault,[49] A. Creusot,[6] A. Criss,[50] J. Cronin,[59] A. Curutiu,[37] S. Dagoret-Campagne,[30] R. Dallier,[36] B. Daniel,[14] S. Dasso,[60,61] K. Daumiller,[33] B. R. Dawson,[28] R. M. de Almeida,[62] M. De Domenico,[52] C. De Donato,[12] S. J. de Jong,[16,58] G. De La Vega,[63] W. J. M. de Mello Junior,[14] J. R. T. de Mello Neto,[41] I. De Mitri,[54] V. de Souza,[64] K. D. de Vries,[65] L. del Peral,[38] M. del Río,[40,57] O. Deligny,[66] H. Dembinski,[22] N. Dhital,[56] C. Di Giulio,[40,67] M. L. Díaz Castro,[29] P. N. Diep,[68] F. Diogo,[1] C. Dobrigkeit,[14] W. Docters,[65] J. C. D'Olivo,[12] P. N. Dong,[66,68] A. Dorofeev,[43] J. C. dos Anjos,[29] M. T. Dova,[19] D. D'Urso,[15] I. Dutan,[37] J. Ebr,[39] R. Engel,[33] M. Erdmann,[69] C. O. Escobar,[4,14] J. Espadanal,[1] A. Etchegoyen,[10,11] P. Facal San Luis,[59] H. Falcke,[16,70] G. Farrar,[8] A. C. Fauth,[14] N. Fazzini,[4] A. P. Ferguson,[49] B. Fick,[56] A. Filevich,[11] A. Filipčič,[71,72] S. Fliescher,[69] C. E. Fracchiolla,[43] E. D. Fraenkel,[65] O. Fratu,[26] U. Fröhlich,[25] B. Fuchs,[22] R. Gaior,[21] R. F. Gamarra,[11] S. Gambetta,[73] B. García,[63] S. T. Garcia Roca,[13] D. Garcia-Gamez,[30] D. Garcia-Pinto,[20] A. Gascon Bravo,[48] H. Gemmeke,[27] P. L. Ghia,[21] M. Giller,[74] J. Gitto,[63] H. Glass,[4] M. S. Gold,[34] G. Golup,[7] F. Gomez Albarracin,[19] M. Gómez Berisso,[7] P. F. Gómez Vitale,[24] P. Gonçalves,[1] J. G. Gonzalez,[33] B. Gookin,[43] A. Gorgi,[2] P. Gouffon,[5] E. Grashorn,[9] S. Grebe,[16,58] N. Griffith,[9] M. Grigat,[69] A. F. Grillo,[75] Y. Guardincerri,[61] F. Guarino,[15] G. P. Guedes,[76] P. Hansen,[19] D. Harari,[7] T. A. Harrison,[28] J. L. Harton,[43] A. Haungs,[33] T. Hebbeker,[69] D. Heck,[33] A. E. Herve,[28] C. Hojvat,[4] N. Hollon,[59] V. C. Holmes,[28] P. Homola,[42] J. R. Hörandel,[16] P. Horvath,[77] M. Hrabovský,[39,77] D. Huber,[22] T. Huege,[33] A. Insolia,[52] F. Ionita,[59] A. Italiano,[52] C. Jarne,[19] S. Jiraskova,[16] M. Josebachuili,[11] K. Kadija,[18] K. H. Kampert,[35] P. Karhan,[78] P. Kasper,[4] I. Katkov,[22] B. Kégl,[30] B. Keilhauer,[33] A. Keivani,[79] J. L. Kelley,[16] E. Kemp,[14] R. M. Kieckhafer,[56] H. O. Klages,[33] M. Kleifges,[27] J. Kleinfeller,[33,57] J. Knapp,[46] D.-H. Koang,[23] K. Kotera,[59] N. Krohm,[35] O. Krömer,[27] D. Kruppke-Hansen,[35] F. Kuehn,[4] D. Kuempel,[25,69] J. K. Kulbartz,[80] N. Kunka,[27] G. La Rosa,[53] C. Lachaud,[6] D. LaHurd,[49] L. Latronico,[2] R. Lauer,[34] P. Lautridou,[36]

S. Le Coz,[23] M. S. A. B. Leão,[81] D. Lebrun,[23] P. Lebrun,[4] M. A. Leigui de Oliveira,[81]
A. Letessier-Selvon,[21] I. Lhenry-Yvon,[66] K. Link,[22] R. López,[82] A. Lopez Agüera,[13]
K. Louedec,[23,30] J. Lozano Bahilo,[48] L. Lu,[46] A. Lucero,[11] M. Ludwig,[22] H. Lyberis,[41,66]
M. C. Maccarone,[53] C. Macolino,[21] S. Maldera,[2] D. Mandat,[39] P. Mantsch,[4] A. G. Mariazzi,[19]
J. Marin,[2,57] V. Marin,[36] I. C. Maris,[21] H. R. Marquez Falcon,[83] G. Marsella,[84] D. Martello,[54]
L. Martin,[36] H. Martinez,[85] O. Martínez Bravo,[82] H. J. Mathes,[33] J. Matthews,[79,86]
J. A. J. Matthews,[34] G. Matthiae,[40] D. Maurel,[33] D. Maurizio,[55] P. O. Mazur,[4]
G. Medina-Tanco,[12] M. Melissas,[22] D. Melo,[11] E. Menichetti,[55] A. Menshikov,[27] P. Mertsch,[87]
C. Meurer,[69] S. Mićanović,[18] M. I. Micheletti,[88] I. A. Minaya,[20] L. Miramonti,[51]
L. Molina-Bueno,[48] S. Mollerach,[7] M. Monasor,[59] D. Monnier Ragaigne,[30] F. Montanet,[23]
B. Morales,[12] C. Morello,[2] E. Moreno,[82] J. C. Moreno,[19] M. Mostafá,[43] C. A. Moura,[81]
M. A. Muller,[14] G. Müller,[69] M. Münchmeyer,[21] R. Mussa,[55] G. Navarra,[2] J. L. Navarro,[48]
S. Navas,[48] P. Necesal,[39] L. Nellen,[12] A. Nelles,[16,58] J. Neuser,[35] P. T. Nhung,[68] M. Niechciol,[25]
L. Niemietz,[35] N. Nierstenhoefer,[35] D. Nitz,[56] D. Nosek,[78] L. Nožka,[39] J. Oehlschläger,[33]
A. Olinto,[59] M. Ortiz,[20] N. Pacheco,[38] D. Pakk Selmi-Dei,[14] M. Palatka,[39] J. Pallotta,[89]
N. Palmieri,[22] G. Parente,[13] E. Parizot,[6] A. Parra,[13] S. Pastor,[90] T. Paul,[91] M. Pech,[39]
J. Pękala,[42] R. Pelayo,[13,82] I. M. Pepe,[92] L. Perrone,[84] R. Pesce,[73] E. Petermann,[93]
S. Petrera,[67] A. Petrolini,[73] Y. Petrov,[43] C. Pfendner,[3] R. Piegaia,[61] T. Pierog,[33]
P. Pieroni,[61] M. Pimenta,[1] V. Pirronello,[52] M. Platino,[11] M. Plum,[69] V. H. Ponce,[7]
M. Pontz,[25] A. Porcelli,[33] P. Privitera,[59] M. Prouza,[39] E. J. Quel,[89] S. Querchfeld,[35]
J. Rautenberg,[35] O. Ravel,[36] D. Ravignani,[11] B. Revenu,[36] J. Ridky,[39] S. Riggi,[13]
M. Risse,[25] P. Ristori,[89] H. Rivera,[51] V. Rizi,[67] J. Roberts,[8] W. Rodrigues de Carvalho,[13]
G. Rodriguez,[13] I. Rodriguez Cabo,[13] J. Rodriguez Martino,[57] J. Rodriguez Rojo,[57]
M. D. Rodríguez-Frías,[38] G. Ros,[38] J. Rosado,[20] T. Rossler,[77] M. Roth,[33]
B. Rouillé-d'Orfeuil,[59] E. Roulet,[7] A. C. Rovero,[60] C. Rühle,[27] A. Saftoiu,[44]
F. Salamida,[66] H. Salazar,[82] F. Salesa Greus,[43] G. Salina,[40] F. Sánchez,[11] C. E. Santo,[1]
E. Santos,[1] E. M. Santos,[41] F. Sarazin,[94] B. Sarkar,[35] S. Sarkar,[87] R. Sato,[57] N. Scharf,[69]
V. Scherini,[51] H. Schieler,[33] P. Schiffer,[69,80] A. Schmidt,[27] O. Scholten,[65]
H. Schoorlemmer,[16,58] J. Schovancova,[39] P. Schovánek,[39] F. Schröder,[33]
S. Schulte,[69] D. Schuster,[94] S. J. Sciutto,[19] M. Scuderi,[52] A. Segreto,[53] M. Settimo,[25]
A. Shadkam,[79] R. C. Shellard,[29] I. Sidelnik,[11] G. Sigl,[80] O. Sima,[95] A. Śmiałkowski,[74]
R. Šmída,[33] G. R. Snow,[93] P. Sommers,[50] J. Sorokin,[28] H. Spinka,[4,96] R. Squartini,[57]
Y. N. Srivastava,[91] S. Stanic,[72] J. Stapleton,[9] J. Stasielak,[42] M. Stephan,[69] A. Stutz,[23]
F. Suarez,[11] T. Suomijärvi,[66] A. D. Supanitsky,[60] T. Šuša,[18] M. S. Sutherland,[79] J. Swain,[91]
Z. Szadkowski,[74] M. Szuba,[33] A. Tapia,[11] M. Tartare,[23] O. Taşcău,[35] R. Tcaciuc,[25]
N. T. Thao,[68] D. Thomas,[43] J. Tiffenberg,[61] C. Timmermans,[16,58] W. Tkaczyk,[74]
C. J. Todero Peixoto,[64] G. Toma,[44] L. Tomankova,[39] B. Tomé,[1] A. Tonachini,[55]
P. Travnicek,[39] D. B. Tridapalli,[5] G. Tristram,[6] E. Trovato,[52] M. Tueros,[13] R. Ulrich,[33]
M. Unger,[33] M. Urban,[30] J. F. Valdés Galicia,[12] I. Valiño,[13] L. Valore,[15] A. M. van den Berg,[65]
E. Varela,[82] B. Vargas Cárdenas,[12] J. R. Vázquez,[20] R. A. Vázquez,[13] D. Veberič,[71,72]
V. Verzi,[40] J. Vicha,[39] M. Videla,[63] L. Villaseñor,[83] H. Wahlberg,[19] P. Wahrlich,[28]
O. Wainberg,[10,11] D. Walz,[69] A. A. Watson,[46] M. Weber,[27] K. Weidenhaupt,[69] A. Weindl,[33]
F. Werner,[33] S. Westerhoff,[3] B. J. Whelan,[28] A. Widom,[91] G. Wieczorek,[74] L. Wiencke,[94]
B. Wilczyńska,[42] H. Wilczyński,[42] M. Will,[33] C. Williams,[59] T. Winchen,[69] M. Wommer,[33]
B. Wundheiler,[11] T. Yamamoto,[59,97] T. Yapici,[56] P. Younk,[25,98] G. Yuan,[79] A. Yushkov,[13]
B. Zamorano Garcia,[48] E. Zas,[13] D. Zavrtanik,[71,72] M. Zavrtanik,[71,72] I. Zaw,[8,99] A. Zepeda,[85]
Y. Zhu,[27] M. Zimbres Silva,[14,35] and M. Ziolkowski[25]

[1] *LIP and Instituto Superior Técnico, Technical University of Lisbon, Lisboa, Portugal*
[2] *Istituto di Fisica dello Spazio Interplanetario (INAF), Università di Torino and Sezione INFN, Torino, Italy*
[3] *University of Wisconsin, Madison, WI, USA*
[4] *Fermilab, Batavia, IL, USA*
[5] *Universidade de São Paulo, Instituto de Física, São Paulo, SP, Brazil*
[6] *Laboratoire AstroParticule et Cosmologie (APC), Université Paris 7, CNRS-IN2P3, Paris, France*
[7] *Centro Atómico Bariloche and Instituto Balseiro (CNEA-UNCuyo-CONICET), San Carlos de Bariloche, Argentina*
[8] *New York University, New York, NY, USA*
[9] *Ohio State University, Columbus, OH, USA*
[10] *Universidad Tecnológica Nacional-Facultad Regional Buenos Aires, Buenos Aires, Argentina*
[11] *Instituto de Tecnologías en Detección y Astropartículas (CNEA, CONICET, UNSAM), Buenos Aires, Argentina*
[12] *Universidad Nacional Autonoma de Mexico, Mexico, DF, Mexico*
[13] *Universidad de Santiago de Compostela, Santiago de Compostela, Spain*
[14] *Universidade Estadual de Campinas, IFGW, Campinas, SP, Brazil*
[15] *Università di Napoli "Federico II" and Sezione INFN, Napoli, Italy*
[16] *IMAPP, Radboud University Nijmegen, Nijmegen, The Netherlands*
[17] *University of Wisconsin, Milwaukee, WI, USA*
[18] *Rudjer Bošković Institute, 10000 Zagreb, Croatia*
[19] *IFLP, Universidad Nacional de La Plata and CONICET, La Plata, Argentina*
[20] *Universidad Complutense de Madrid, Madrid, Spain*
[21] *Laboratoire de Physique Nucléaire et de Hautes Energies (LPNHE), Universités Paris 6 et Paris 7, CNRS-IN2P3, Paris, France*
[22] *Karlsruhe Institute of Technology-Campus Süd-Institut für Experimentelle Kernphysik (IEKP), Karlsruhe, Germany*
[23] *Laboratoire de Physique Subatomique et de Cosmologie (LPSC), Université Joseph Fourier, INPG, CNRS-IN2P3, Grenoble, France*
[24] *Observatorio Pierre Auger and Comisión Nacional de Energía Atómica, Malargüe, Argentina*
[25] *Universität Siegen, Siegen, Germany*
[26] *University Politehnica of Bucharest, Bucharest, Romania*
[27] *Karlsruher Institut für Technologie-Campus Nord-Institut für Prozessdatenverarbeitung und Elektronik, Karlsruhe, Germany*
[28] *University of Adelaide, Adelaide, SA, Australia*
[29] *Centro Brasileiro de Pesquisas Fisicas, Rio de Janeiro, RJ, Brazil*
[30] *Laboratoire de l'Accélérateur Linéaire (LAL), Université Paris 11, CNRS-IN2P3, Orsay, France*
[31] *Universidade Estadual do Sudoeste da Bahia, Vitoria da Conquista, BA, Brazil*
[32] *University of Maryland, College Park, MD, USA*
[33] *Karlsruhe Institute of Technology-Campus North-Institut für Kernphysik, Karlsruhe, Germany*
[34] *University of New Mexico, Albuquerque, NM, USA*
[35] *Bergische Universität Wuppertal, Wuppertal, Germany*
[36] *SUBATECH, École des Mines de Nantes, CNRS-IN2P3, Université de Nantes, Nantes, France*
[37] *Max-Planck-Institut für Radioastronomie, Bonn, Germany*
[38] *Universidad de Alcalá, Alcalá de Henares, Madrid, Spain*
[39] *Institute of Physics of the Academy of Sciences of the Czech Republic, Prague, Czech Republic*
[40] *Università di Roma II "Tor Vergata" and Sezione INFN, Roma, Italy*
[41] *Instituto de Física, Universidade Federal do Rio de Janeiro, Rio de Janeiro, RJ, Brazil*
[42] *Institute of Nuclear Physics PAN, Krakow, Poland*
[43] *Colorado State University, Fort Collins, CO, USA*
[44] *Horia Hulubei National Institute for Physics and Nuclear Engineering, Bucharest-Magurele, Romania*
[45] *Colorado State University, Pueblo, CO, USA*
[46] *School of Physics and Astronomy, University of Leeds, Leeds, UK*
[47] *Université de Lausanne, Lausanne, Switzerland*
[48] *Universidad de Granada & C.A.F.P.E., Granada, Spain*
[49] *Case Western Reserve University, Cleveland, OH, USA*
[50] *Pennsylvania State University, University Park, PA, USA*
[51] *Università di Milano and Sezione INFN, Milan, Italy*
[52] *Università di Catania and Sezione INFN, Catania, Italy*
[53] *Istituto di Astrofisica Spaziale e Fisica Cosmica di Palermo (INAF), Palermo, Italy*
[54] *Dipartimento di Fisica dell'Università del Salento and Sezione INFN, Lecce, Italy*
[55] *Università di Torino and Sezione INFN, Torino, Italy*
[56] *Michigan Technological University, Houghton, MI, USA*
[57] *Observatorio Pierre Auger, Malargüe, Argentina*
[58] *Nikhef, Science Park, Amsterdam, The Netherlands*
[59] *Enrico Fermi Institute, University of Chicago, Chicago, IL, USA*

[60]Instituto de Astronomía y Física del Espacio (CONICET-UBA), Buenos Aires, Argentina
[61]Departamento de Física, FCEyN, Universidad de Buenos Aires y CONICET, Buenos Aires, Argentina
[62]Universidade Federal Fluminense, EEIMVR, Volta Redonda, RJ, Brazil
[63]Faculty Mendoza (CONICET/CNEA), National Technological University, Mendoza, Argentina
[64]Instituto de Física, Universidade de São Paulo, São Carlos, SP, Brazil
[65]Kernfysisch Versneller Instituut, University of Groningen, Groningen, The Netherlands
[66]Institut de Physique Nucléaire d'Orsay (IPNO), Université Paris 11, CNRS-IN2P3, Orsay, France
[67]Università dell'Aquila and INFN, L'Aquila, Italy
[68]Institute for Nuclear Science and Technology (INST), Hanoi, Vietnam
[69]III. Physikalisches Institut A, RWTH Aachen University, Aachen, Germany
[70]ASTRON, Dwingeloo, The Netherlands
[71]J. Stefan Institute, Ljubljana, Slovenia
[72]Laboratory for Astroparticle Physics, University of Nova Gorica, Nova Gorica, Slovenia
[73]Dipartimento di Fisica dell'Università and INFN, Genova, Italy
[74]University of Łódź, Łódź, Poland
[75]INFN, Laboratori Nazionali del Gran Sasso, Assergi, L'Aquila, Italy
[76]Universidade Estadual de Feira de Santana, Feira de Santana, Brazil
[77]RCPTM, Palacky University, Olomouc, Czech Republic
[78]Institute of Particle and Nuclear Physics, Faculty of Mathematics and Physics, Charles University, Prague, Czech Republic
[79]Louisiana State University, Baton Rouge, LA, USA
[80]Universität Hamburg, Hamburg, Germany
[81]Universidade Federal do ABC, Santo André, SP, Brazil
[82]Benemérita Universidad Autónoma de Puebla, Puebla, Mexico
[83]Universidad Michoacana de San Nicolas de Hidalgo, Morelia, Michoacan, Mexico
[84]Dipartimento di Ingegneria dell'Innovazione dell'Università del Salento and Sezione INFN, Lecce, Italy
[85]Centro de Investigación y de Estudios Avanzados del IPN (CINVESTAV), México, DF, Mexico
[86]Southern University, Baton Rouge, LA, USA
[87]Rudolf Peierls Centre for Theoretical Physics, University of Oxford, Oxford, UK
[88]Instituto de Física Rosario (IFIR), CONICET/U.N.R. and Facultad de Ciencias Bioquímicas y Farmacéuticas U.N.R., Rosario, Argentina
[89]Centro de Investigaciones en Láseres y Aplicaciones, CITEDEF and CONICET, San Carlos de Bariloche, Argentina
[90]Instituto de Física Corpuscular, CSIC-Universitat de València, Valencia, Spain
[91]Northeastern University, Boston, MA, USA
[92]Universidade Federal da Bahia, Salvador, BA, Brazil
[93]University of Nebraska, Lincoln, NE, USA
[94]Colorado School of Mines, Golden, CO, USA
[95]Physics Department, University of Bucharest, Bucharest, Romania
[96]Argonne National Laboratory, Argonne, IL, USA
[97]Konan University, Kobe, Japan
[98]Los Alamos National Laboratory, Los Alamos, NM, USA
[99]NYU Abu Dhabi, Abu Dhabi, UAE

Correspondence should be addressed to The Pierre Auger Collaboration; auger_spokesperson@fnal.gov

Received 15 February 2012; Accepted 25 June 2012

Academic Editor: Kara Hoffman

The observation of ultrahigh energy neutrinos (UHEνs) has become a priority in experimental astroparticle physics. UHEνs can be detected with a variety of techniques. In particular, neutrinos can interact in the atmosphere (downward-going ν) or in the Earth crust (Earth-skimming ν), producing air showers that can be observed with arrays of detectors at the ground. With the surface detector array of the Pierre Auger Observatory we can detect these types of cascades. The distinguishing signature for neutrino events is the presence of very inclined showers produced close to the ground (i.e., after having traversed a large amount of atmosphere). In this work we review the procedure and criteria established to search for UHEνs in the data collected with the ground array of the Pierre Auger Observatory. This includes Earth-skimming as well as downward-going neutrinos. No neutrino candidates have been found, which allows us to place competitive limits to the diffuse flux of UHEνs in the EeV range and above.

1. Introduction

The observation of ultrahigh energy cosmic rays (UHECR) of energy 1–100 EeV (10^{18}–10^{20} eV) has stimulated much experimental as well as theoretical activity in the field of Astroparticle Physics [1, 2]. Although many mysteries remain to be solved, such as the origin of the UHECRs, their production mechanism and composition, we know that it is very difficult to produce these energetic particles without associated fluxes of ultrahigh energy neutrinos (UHEνs) [3].

In the so-called "bottom-up" models, protons and nuclei are accelerated in astrophysical shocks, where pions are believed to be produced by cosmic ray interactions with matter or radiation at the source [4]. In the so-called "top-down" scenarios, protons and neutrons are produced from quark and gluon fragmentation, a mechanism which is known to produce much more pions than nucleons [5]. Furthermore, protons and nuclei also produce pions in their unavoidable interactions responsible for the Greisen-Zatsepin-Kuzmin (GZK) cutoff [6–8]. The flux of UHECRs above $\sim 5 \times 10^{19}$ eV is known to be largely suppressed with respect to that at lower energies, a feature seen in the UHECR spectrum [9–11] that is compatible with the interaction of UHECRs with the cosmic microwave background (CMB) radiation. If the primaries are protons, the interaction responsible for the GZK effect is photopion production, and the decays of the charged pions produce UHE neutrinos. However, their fluxes are uncertain [4], and if the primaries are heavy nuclei, the UHEν yield would be strongly suppressed [12].

The observation of UHE neutrinos could provide important hints to the origin of UHECRs [13, 14]. Unlike cosmic rays, neutrinos point directly to the source where they were produced, without being deflected by galactic and extragalactic magnetic fields. Unlike photons they travel undisturbed from the sources carrying a footprint of the production model.

High energy neutrinos can be detected with a variety of techniques [15, 16]. In particular, they can be observed with arrays of detectors at ground level that are currently being used to measure extensive showers produced by cosmic rays [17]. The main challenge in this technique lies in separating showers initiated by neutrinos from those induced by regular cosmic rays. It was suggested in the 1970s that this could be done at high zenith angles [18] because the atmosphere slant depth provides a quite large target for neutrino interactions. The idea is that neutrinos, having very small cross-sections, can interact at any point along their trajectories, while protons, nuclei, or photons interact shortly after entering the atmosphere. The signature for neutrino events is thus inclined showers that interact deep in the atmosphere.

Inclined showers were first observed in the 1960s by several groups [19–22]. With the surface detector array (SD) of the Pierre Auger Observatory [23] we can detect inclined showers and identify neutrinos with energies typically above 0.1 EeV. There are two ways of performing this task.

(1) Neutrinos of all flavours can collide with nuclei in the atmosphere and induce an extensive air shower close to the ground [24, 25]. In this so-called "downward-going" neutrino channel, both charged current (CC) and neutral-current (NC) interactions contribute to the neutrino event rate.

(2) Neutrinos of tau flavour (ν_τ) are expected to be most sensitively observed through the detection of showers induced by the decay products of an emerging τ lepton, after the propagation and interaction of an upward-going ν_τ inside the Earth [26, 27]. This "Earth-skimming" channel benefits from the long range of the τ lepton (~10 km for the shower energies relevant in this analysis) which sets the scale of the effective volume. Only charged-current interactions of ν_τ are relevant in this case.

In both the Earth-skimming and downward-going channels the showers can be identified and separated from cosmic ray induced showers with the SD of the Pierre Auger Observatory if the zenith angle is large enough, typically larger than ~65°–75°. A number of properties of the shower front, mostly stemming from the time distribution of the shower particles, can be used to distinguish neutrino-induced showers. As shown in Section 5, even though the criteria to identify neutrinos in both channels being based on similar ideas and variables, two different analyses were designed. The main reason for that concerns background reduction. The Earth-skimming neutrino search is restricted to a very narrow angular range where the background of nucleonic showers is expected to be very small. On the other hand, in the broader angular range of the downward-going neutrino search the background contamination is expected to be larger, and the selection criteria need to be more restrictive. This calls for specific algorithms and methods, capable of optimizing the separation of neutrino-induced showers from nucleonic ones as will be explained later in the paper.

In this work we review the procedure to search for UHEνs with the SD of the Auger Observatory, for both the Earth-skimming and downward-going channels. In Section 2 we give a brief overview of the SD of the Pierre Auger Observatory. In Section 3 we concentrate on the general strategy to search for UHEνs. Section 4 is devoted to describe the simulations of neutrino-induced showers crucial to establish selection criteria and to compute the exposure to UHEνs which is reported in Section 6. In Section 5 we give a detailed description of the neutrino selection criteria. When these criteria are applied blindly to the data collected at the SD no candidates are found. The resulting limits to the diffuse flux of UHEνs are presented in Section 7. Finally, in Section 8 we summarize the paper and give some prospects for future observations.

2. The Pierre Auger Observatory

The Pierre Auger Observatory [23] is a hybrid UHECR detector combining an array of particle detectors at ground level, and 24 fluorescence telescopes housed in four buildings, for redundancy and calibration. It is located near the town of Malargüe, in the province of Mendoza in Argentina. In this paper we focus on the surface detector array [23, 28] which is briefly described in the following.

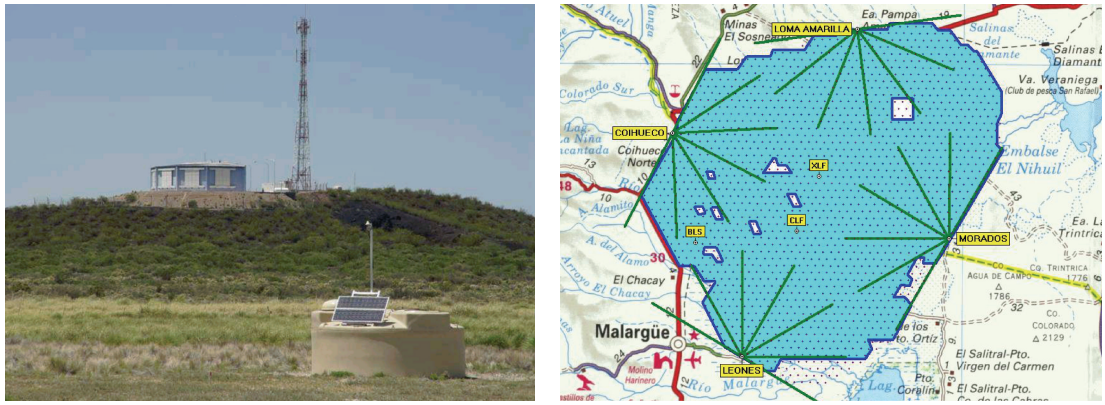

(a) (b)

Figure 1: (a) One of the ~1600 water Cherenkov stations that constitute the surface detector array of the Pierre Auger Observatory (forefront), and one of the four fluorescence buildings housing six of the 24 fluorescence telescopes (background). (b) Layout of the SD array with ~1600 water Cherenkov stations (depicted as dots), spread over a surface of ~3000 km^2 (blue area), with a distance between stations of 1.5 km. The four fluorescence buildings at the edges of the observatory are also indicated.

2.1. The Surface Detector Array. The surface detector array [28] consists of water Cherenkov detectors in the form of cylinders of 3.6 m diameter and 1.2 m height, each containing 12 tonnes of purified water. Charged particles entering the station emit Cherenkov light which is reflected at the walls by a diffusive Tyvek liner, and collected by three 9-inch photomultiplier tubes (PMT) at the top surface and in optical contact with the water. The PMT signals are sampled by flash analog to digital converters (FADC) with a time resolution of 25 ns. Each station is regularly monitored and calibrated in units of vertical equivalent muons (VEM) corresponding to the signal produced by a muon traversing the tank vertically through its center [29]. In Figure 1 we show a picture of one of the water Cherenkov stations. The stations are autonomous, with all their components (PMTs, local processor, GPS receiver, and radio system) powered by batteries coupled to solar panels. Once installed, the local stations work continuously without external intervention.

The SD was completed in 2008. There are ~1600 water stations arranged in a triangular grid with 1.5 km spacing between them, spanning an almost flat surface of ~3000 km^2, at an approximate altitude of 1400 m above sea level, or equivalently an atmospheric depth $X_{\text{ground}} = 880\ \text{g cm}^{-2}$. The layout of the SD array is sketched in the right panel of Figure 1.

2.2. Surface Detector Trigger. The stations transmit information by conventional radio links to the Central Data Acquisition System (CDAS) located in Malargüe. There are two types of trigger conditions. A local trigger at the level of an individual station (second order or T2 trigger), and a global trigger (third order or T3 trigger). The T2 trigger condition is the logical OR of two conditions: either a given threshold signal (3.2 VEM) is passed in at least one time bin of the FADC trace—the so-called "Threshold trigger"— or a somewhat lower threshold (0.2 VEM) is passed in at least 13 bins within a 3 μs time window (i.e., 120 bins)—the so-called "Time-over-Threshold (ToT) trigger." The ToT condition was designed to trigger on signals broad in time, characteristic of the early stages of the development of an extensive air shower, and is crucial for neutrino identification as explained below. The data acquisition system receives the local T2 triggers and builds a global T3 trigger requiring a relatively compact configuration of at least three local stations compatible in time, each satisfying the ToT trigger, or four triggered stations with any type of T2 trigger [30]. With the completed array, the global T3 trigger rate is about two events per minute, one third being actual shower events at energies above 3×10^{17} eV.

3. Generalities of UHE Neutrino Search

With the SD of the Pierre Auger Observatory we can detect and identify UHE neutrinos in the EeV range and above [31–33]. The main challenge from the experimental point of view is to identify neutrino-induced showers in the large background of showers initiated by nucleonic cosmic rays. The concept for identification is relatively simple. While protons, heavier nuclei and even photons interact shortly after entering the atmosphere, neutrinos can generate showers initiated deeply into the atmosphere. When considering vertical showers, even the ones initiated by protons or heavy nuclei have a considerable amount of electromagnetic component at the ground ("young" shower front). However, when looking at high zenith angles ($\theta > 75^\circ$) the atmosphere is thick enough (thicker than about three vertical atmospheres) so that the cosmic rays interacting high in the atmosphere have shower fronts dominated by muons at ground ("old" shower front). A neutrino with $\theta > 75^\circ$ interacting deep will present a young shower front and, consequently, can be distinguished.

At the SD level, young showers induce signals spread in time over hundreds of nano-seconds in a fraction of the stations triggered by the shower, while old showers induce narrow signals spreading over typically tens of nano-seconds in practically all the stations of the event. With the 25 ns time resolution of the FADC of the water Cherenkov stations,

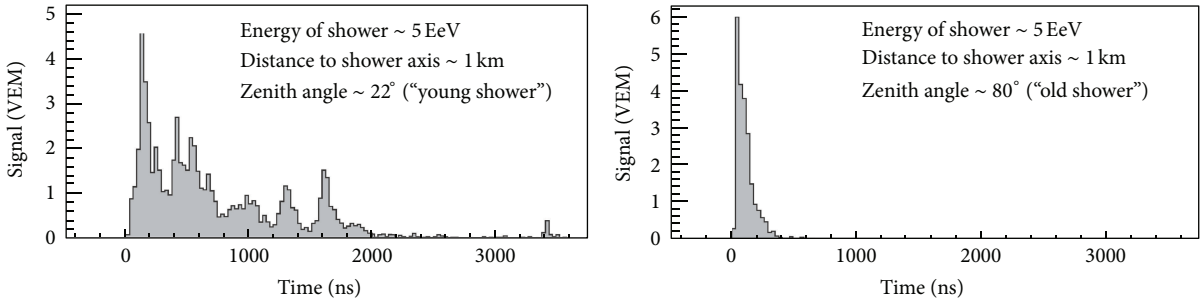

FIGURE 2: FADC traces of stations at 1 km from the shower core for two real showers of 5 EeV. (a) shower arriving in the early stages of development ("young" shower). (b) "old" extensive air shower ($\theta \sim 80^\circ$).

the distinction between traces induced by young and old shower fronts can be easily accomplished. In Figure 2 we show an example of those two types of traces.

With this simple idea, we can search for two types of neutrino-induced showers at the surface detector array of the Pierre Auger Observatory, as follows.

(1) Earth-skimming showers induced by tau neutrinos (ν_τ) that travel in the upward direction with respect to the vertical to ground. ν_τ can skim the Earth's crust and interact relatively close to the surface inducing a tau lepton which escapes the Earth and decays in flight in the atmosphere, close to the SD. Typically, only Earth-skimming ν_τ-induced showers with zenith angles $90^\circ < \theta < 95^\circ$ may be identified.

(2) Showers initiated by any neutrino flavour moving down at large angles with respect to the vertical at ground that interact in the atmosphere close to the surface detector array. We include here showers induced by ν_τ interacting in the mountains surrounding the Pierre Auger Observatory. Although this latter process is exactly equivalent to the "Earth-skimming" mechanism, it is included in this class because such showers are also going downwards. In the following we will refer to all these types of showers as "downward-going" ν-induced showers. In this paper we restrict ourselves to downward-going ν-induced showers with zenith angles $75^\circ \leq \theta \leq 90^\circ$.

In Figure 3 we show a pictorial representation of the different types of inclined showers that can be detected.

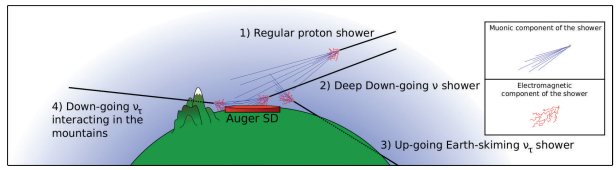

FIGURE 3: Pictorial representation of the different types of inclined showers that can be detected at the surface detector array of the Pierre Auger Observatory. (1) An inclined shower induced by a proton interacting high in the atmosphere whose electromagnetic component is absorbed and only the muons reach the detector. Inclined showers presenting significant electromagnetic component at the detector level: (2) a deep downward-going ν-induced shower; (3) an Earth-skimming ν_τ interacting in the Earth crust and producing an upward-going τ lepton that decays in flight and induces a shower in the atmosphere; and (4) a ν_τ interacting in the mountains, producing a downward-going τ lepton that decays close to the detector and initiates a shower.

4. Simulation of Neutrino Showers

Monte Carlo simulations of neutrino-induced showers are crucial to establishing identification criteria and computing the acceptance of the SD to UHEνs. The whole simulation chain is divided into three stages.

(1) High energy processes:

(a) the ν-nucleon interaction in the atmosphere for downward-going neutrinos is simulated with HERWIG [34]. The output of HERWIG includes the types, energies, and momenta of the secondary particles produced for both charged (CC) and neutral current (NC) neutrino interactions (see Figure 4 for a pictorial summary of all the channels considered in this work);

(b) in the case of ν_τ CC interactions, the τ lepton propagation in the Earth and/or in the atmosphere is simulated with a dedicated, fast, and flexible code which allows us to easily study the influence on the outgoing τ lepton flux of different ν_τ interaction cross sections, τ energy loss models, and so forth. The simulation of the decay of the τ (when necessary) is performed with the TAUOLA package [35].

(2) Shower development in the atmosphere: The AIRES Monte Carlo code [36] is used to propagate the particles produced in a high energy ν interaction, or in the decay of a τ lepton. The types, energies, momenta, and times of the particles reaching the SD level are obtained.

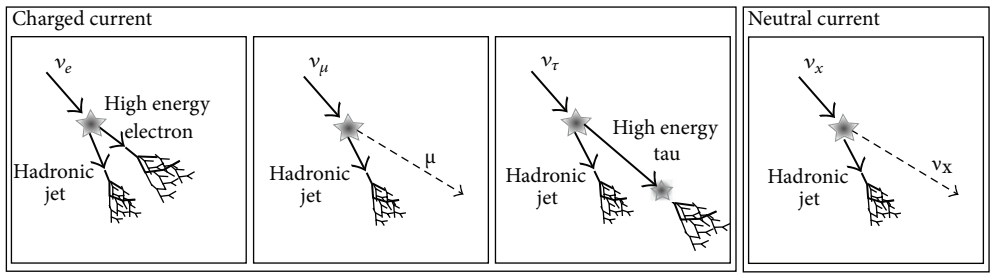

Figure 4: Sketch of the different types of showers induced by UHE neutrinos. All the channels depicted contribute to the neutrino event rate due to downward-going ν induced showers.

(3) Surface detector array simulation: This is performed with the $\overline{\text{Off}}\underline{\text{line}}$ software [37]. Firstly, particles reaching a surface detector station are injected into the station, and with the aid of GEANT4 [38] the amount of Cherenkov light produced in water is calculated. Then the FADC traces of the PMT signals are obtained, and the total signal due to the particles entering the station, as well as several quantities characterizing the FADC trace which will be relevant for neutrino identification are computed (see below). Also both the local trigger condition (T2—either threshold or ToT), and the global trigger condition (T3) are applied to the simulated events in the same way as for collected data.

The phase space of the simulations—namely, neutrino energy, zenith angle of incidence, interaction depth in the atmosphere for downward-going neutrinos, and altitude of the τ decay in the case of Earth-skimming ν_τ—spans a sufficiently wide range of numerical values as to guarantee that at the edges of the phase space none of the simulated showers fulfills the global trigger conditions. This is taken as a clear indication that a complete sample of showers has been produced without introducing any bias and therefore that the Monte Carlo sample correctly represents the characteristic of showers that could trigger the SD of the Pierre Auger Observatory. For the Earth-skimming channel, showers were simulated at zenith angles between 90.1° and 95.9° and at an altitude of the decay point above the Pierre Auger Observatory up to 2500 m. In the case of downward-going neutrinos, simulations were performed at zenith angles in the range 75°–89°.

5. Identifying Neutrino-Induced Showers

As stated above, the selection of potential neutrino-induced showers (neutrino candidates) is based on two steps.

(1) Firstly, we select among the data collected at the SD of the Pierre Auger Observatory those events that arrive in inclined directions with respect to the vertical.

(2) Secondly, we select among the inclined events those with FADC traces that are spread in time, indicative of the presence of an inclined shower in the early stage of development, a clear signature of a deeply interacting neutrino triggering the SD.

Although the two steps above are the same for all the neutrino-induced showers searched for at the Pierre Auger Observatory, due to the different nature of Earth-skimming and downward-going neutrino-induced showers, the criteria and selection cuts that are applied to data are slightly different.

5.1. Selection of Inclined Events. First of all, events occurring during periods of data acquisition instabilities [30] are excluded.

For the remaining events the FADC traces of the triggered stations are first "cleaned" to remove accidental signals induced (mainly) by atmospheric muons arriving closely before or after the shower front—produced in showers different than the triggering one and which are below the energy threshold of the Pierre Auger Observatory. The trace-cleaning procedure is detailed in [32]. After that, the start times of the signals in all stations included in the global trigger are requested to be compatible with a plane shower front moving at roughly the speed of light. This compatibility is realized through upper bounds on both, the largest residual and the mean quadratic residual from the planar fit. If the condition is not fulfilled, fits are attempted removing one station; for this operation, the stations are sorted by increasing *quality* (based on the integrated amplitude and the duration of the signal), and the procedure is stopped as soon as a satisfactory solution is found. If none is found, trials are made removing two stations, and so on. The event is accepted if at least three (four) stations in the Earth-skimming (downward-going) case belong to the configuration.

The second step in both channels is the selection of inclined showers. From the pattern (footprint) of stations at ground (see Figure 5) we can extract a length L along the arrival direction of the event (i.e., the main axis of the event) and a width W perpendicular to it characterizing the shape of the footprint (see [32] for complete details). The ratio L/W depends on zenith angle. Vertical events have $L/W \sim 1$ and this ratio increases gradually as the zenith angle increases. Very inclined events typically have elongated patterns on the ground along the direction of arrival, and hence large values of L/W. A cut in L/W is therefore a good selector of inclined events. The exact value of this cut is different

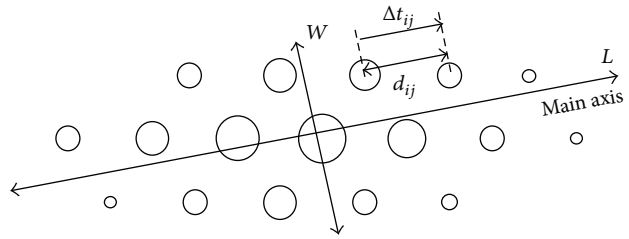

FIGURE 5: Schematic view of the footprint of a shower triggering the surface detector array of the Pierre Auger Observatory. The shower triggers the array from the left to the right of the figure, along the "main axis." The circles represent the position of the stations, with their sizes being proportional to the collected signal in the PMTs. See text for more details.

for downward-going and Earth-skimming events and was determined through Monte Carlo simulations of ν-induced showers performed at different zenith angles. For downward-going events with $\theta > 75^\circ$ the requirement is $L/W > 3$, while for Earth-skimming it is more restrictive $L/W > 5$ since only quasihorizontal showers with largely elongated footprints can trigger the array. The axis of Earth-skimming showers travelling in the upward direction does not intersect ground, contrary to the downward-going showers case. For this reason, we exploit the properties of the footprint generated by the shower particles that deviate laterally from the shower axis and trigger the water Cherenkov stations. (see [32, Figure 3]).

Another indication of inclined events is given by the apparent speed V of the trigger from a station i to a station j, averaged over all pairs (i, j) of stations in the event. This observable denoted as $\langle V \rangle$ is obtained in a straightforward manner from the distance between the stations after projection along the "main axis" of the footprint at ground (d_{ij}) as depicted in Figure 5, and from the difference in trigger times of the stations (Δt_{ij}). Vertical showers have apparent average speeds exceeding the speed of light since all triggers occur at roughly the same time, while in very inclined events $\langle V \rangle$ is concentrated around the speed of light. Moreover its root-mean-square (RMS(V)) is small. For downward-going (Earth-skimming) events $\langle V \rangle$ is required to be below 0.313 m ns^{-1} ($\langle V \rangle \in [0.29, 0.31]$ m ns^{-1}) and RMS(V)/$\langle V \rangle$ < 0.08 (RMS(V) < 0.08 m ns^{-1}). The values of these selection requirements are based on comparisons between data and Monte Carlo simulations. Also, and only for downward-going events, a further quality cut is applied consisting on a simple reconstruction of the zenith angle θ_{rec} and the requirement that $\theta_{\text{rec}} > 75^\circ$ (see [33] for full details).

In the top of Table 1 the cuts applied to the observables used to select inclined events are summarized.

5.2. Selection of Young Showers. Once inclined showers are selected, the next step is to identify young showers among the data collected at the SD of the Pierre Auger Observatory.

To optimize the numerical values of the cuts and tune the algorithms needed to separate neutrino-induced showers from the much larger background of hadronic showers, we divided the whole data sample into two parts (excluding periods of array instability). A fraction of the data (training period) is dedicated to define the selection algorithm. These data are assumed to be overwhelmingly constituted of background showers. The applied procedure is conservative because the presence of neutrinos would result in a more severe definition of the selection criteria. The remaining fraction is not used until the selection procedure is established, and then it is "unblinded" to search for neutrino candidates. In Table 2 we indicate the periods used for training and "blind" search. The blind search period for the Earth-skimming (downward-going) analysis corresponds to an equivalent of ~3.5 yr (~2 yr) of a full surface detector array consisting of 1600 stations working continuously without interruptions.

It is worth remarking that data instead of Monte Carlo simulations of hadronic showers are used to optimize the identification cuts. The first reason for this is that, the composition of the primary UHECR flux—a necessary input in the simulations—is not accurately known. Also, the detector simulation may not account for all possible detector defects and/or fluctuations that may induce events that constitute a background to UHE neutrinos, while they are accounted for in collected data, including those which are not well known, or even not yet diagnosed.

This is the general strategy followed in the search for Earth-skimming ν_τ and downward-going ν-induced showers. However, the two searches differ in several aspects that we detail in the following sections.

5.2.1. Earth-Skimming Analysis. In the Earth-skimming analysis we identify young showers by placing a cut on the fraction of stations in the event that fulfill two conditions: (1) the station passes the ToT local trigger condition and (2) the ratio of the integrated signal over the peak height—the so-called Area-over-Peak (AoP), a variable that carries information on the time spread of the signal—is greater than 1.4. By convention, both the "area" and the "peak" values are normalized to 1 in signals induced by isolated muons.

The aim of both conditions is to identify broad signals in time such as those induced by showers developing close to the array. In particular, with the second condition we reject background signals induced by inclined hadronic showers, in which the muons and their electromagnetic products are concentrated within a short time interval, exhibiting AoP values close to the one measured in signals of isolated muons.

In order to reject inclined hadronic events, at least 60% of the triggered stations in the event are required to fulfill the two conditions above (Table 1). The selection conditions were optimized using data collected during the training period indicated in Table 2. It is important to remark that this is the same selection procedure and training period as in previous publications [31, 32], which is applied in this work to a larger data set. The final choice of the actual values of the neutrino selection cuts was done by requiring zero background events in the training data sample. When the Earth-skimming cuts in Table 1 are applied blindly to the data collected during the search period, no events survived.

Table 1: Observables and numerical values of cuts applied to select *inclined* and *young* showers for Earth-skimming and downward-going neutrinos. See text for explanation.

	Earth-skimming Number of Stations ≥ 3	Downward-going Number of Stations ≥ 4
Inclined showers	—	$\theta_{\rm rec} > 75^\circ$
	$L/W > 5$	$L/W > 3$
	$0.29\,\mathrm{m\,ns^{-1}} < \langle V\rangle < 0.31\,\mathrm{m\,ns^{-1}}$	$\langle V\rangle < 0.313\,\mathrm{m\,ns^{-1}}$
	$\mathrm{RMS}(V) < 0.08\,\mathrm{m\,ns^{-1}}$	$\mathrm{RMS}(V)/\langle V\rangle < 0.08$
Young showers	At least 60% of stations with ToT trigger and AoP > 1.4	Fisher discriminant $\mathcal{F}$ based on Area-over-Peak (AoP)

Table 2: Training and blind search periods for the search for Earth-skimming and downward-going neutrino candidates. In the 3rd row we indicate the equivalent period of time of a full surface detector array. In the 4th row we give the number of candidates found in the search period after unblindly applying the cuts selecting *inclined* and *young* showers (see Table 1). In the 5th row we give the numerical value of the 90% C.L. limit to the normalization k of a diffuse flux of UHE neutrinos assumed to behave with energy as $dN/dE = kE^{-2}$. Systematic uncertainties are included in the value of the limit (see Section 6.3 for details). In the last row we indicate the energy range where the limits apply, typically the energy interval where 90% of the events are expected.

	Earth-skimming	Downward-going
Training period	1 Nov 04–31 Dec 04	1 Jan 04–31 Oct 07
Blind search period	1 Jan 04–31 May 10	1 Nov 07–31 May 10
Equivalent full auger blind search period	3.5 yr	2.0 yr
ν candidates	0	0
Diffuse limit 90% C.L. ($\mathrm{GeV cm^{-2}\,s^{-1}\,sr^{-1}}$)	$k < 3.2 \times 10^{-8}$	$k < 1.7 \times 10^{-7}$
Energy range (EeV)	~0.16–20.0	~0.1–100.0

5.2.2. Downward-Going Analysis. In the search for downward-going events, the discrimination power is optimized with the aid of a multi-variate technique known as the Fisher discriminant method [39]. The method consists on constructing a linear combination of observables denoted as $\mathcal{F}$ which optimizes the separation between two samples of events, in our case background hadronic inclined showers occuring during the downward-going training period (see Table 2), and Monte Carlo simulated ν-induced showers. The method requires as input a set of variables which can discriminate between the two samples. For that purpose we use variables depending on the Area-over-Peak (AoP)—as defined above—of the FADC traces. In the first few stations hit by a deep inclined shower, the typical AoP values range between 3 and 5 (Figure 6(a)).

After training the Fisher method, a good discrimination is found when the following ten variables are used to construct the linear Fisher discriminant variable $\mathcal{F}$: the AoP of the four stations that trigger first (early stations) in each event, their squares, the product of the four AoPs, and a global parameter that measures the asymmetry between the average AoP of the early stations and those triggering last (late stations) of the event.

The product of the AoP of the earliest four stations in the event aims at minimizing the relative weight of an accidentally large AoP produced, for instance, by a single muon which does not belong to the shower front arriving at a station before or after the shower itself. This variable is also a very good discriminator as shown in Figure 6(b). We have also checked in Monte Carlo simulations that neutrino-induced events typically have an asymmetry parameter larger than proton or nucleus-induced showers.

As the shower front is broader at larger distance from the core for both young and old showers, the discrimination is better when splitting the samples according to the number of selected stations N. A Fisher discriminant polynomial was obtained separately for $4 \le N \le 6$, $7 \le N \le 11$, and $N \ge 12$. An excellent separation is achieved for events in each of the three subsamples. The individual AoPs of the first four tanks have the largest weights in the Fisher polynomials. In Figure 7 we show as an example the distribution of $\mathcal{F}$ in the subsample with the smallest number of selected stations (the distributions corresponding to the three subsamples can be found in [33, Figure 7]).

Once the Fisher discriminant $\mathcal{F}$ is defined, the next step is to define a numerical value of $\mathcal{F}$, denoted as $\mathcal{F}_{\rm cut}$, that separates neutrino candidates from regular hadronic showers. One of the advantages of the Fisher discriminant method is that it allows us to estimate the expected rate of background events and, hence, to tune the value of $\mathcal{F}_{\rm cut}$ so that the background is kept at a very low value. This is important given the fact that the expected rate of detected neutrino events will be small. Data in the training period indicated in Table 2 were exploited to produce a reasonable prediction of the background (see [33] for full details). In practice, we fix $\mathcal{F}_{\rm cut}$ so that the estimated number of background events is 1 in 20 yr of data taking by a full Auger SD. With this cut, and for our search sample we have an estimated background of

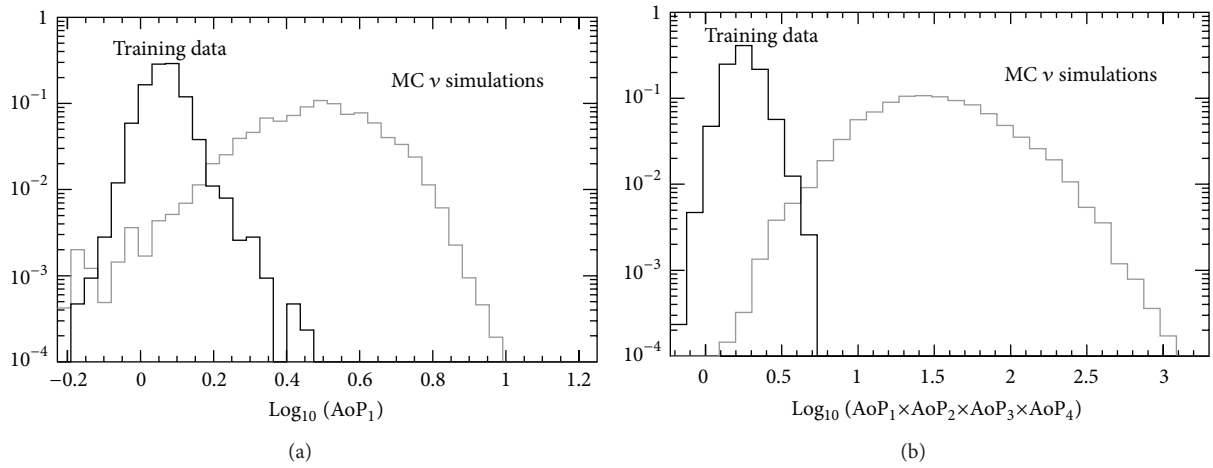

Figure 6: Distributions of the Area-over-Peak (AoP, see text) of the earliest station (a) and of the product of the AoP of the first four stations in the event (b). In each panel we show the distribution of the corresponding variable in background events (i.e., data events in the training sample as indicated in Table 2), and in simulated electron neutrino-charged current events. These are two of the ten variables depending on the AoP used in constructing the multivariate Fisher discriminant linear polynomial to optimize the separation between background and neutrino-induced showers. See text for more details on the remaining eight variables.

0.1 events for each multiplicity class that add up to a total of 0.3 events with a statistical uncertainty of 30%. It is important to remark that this estimate relies on the a priori hypothesis that the background has an exponential distribution in $\mathcal{F}$. Given the fact that we do not have a solid estimation of the actual background, a conservative approach was taken assuming the background is zero, in other words, the estimated 0.3 background events were not used to improve our upper limit on the flux [40] (see Section 7.1).

As exemplified in Figure 7 for the low multiplicity events, the identification cuts reject only ~10% of the simulated neutrino events, and those are mainly neutrinos interacting far from the ground that, being similar to nucleonic-induced showers, are not expected to be identified.

Finally, when the downward-going cuts in Table 1 are applied to the data collected during the search period, no neutrino candidates appeared (see Table 2).

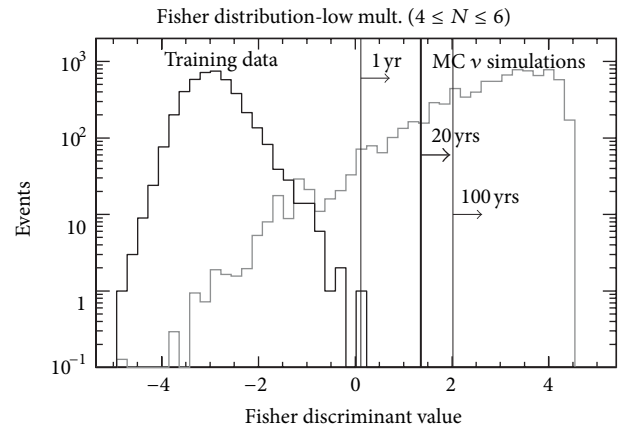

Figure 7: Distribution of the value of the Fisher polynomial ($\mathcal{F}$, see text for details) for events with number of selected stations $4 \leq N \leq 6$. Data in the training period (see Table 2) describe the nucleonic background, while Monte Carlo simulated downward-going neutrinos correspond to the signal. The vertical lines indicate $\mathcal{F}_{\text{cut}}$ needed to expect 1 event in the labeled periods of time (full SD array).

6. Exposure to UHE Neutrinos

6.1. Neutrino Identification Efficiencies. With the criteria to select neutrino-induced showers indicated in Table 1, we obtain a relatively large identification efficiency both for Earth-skimming ν_τ and downward-going ν-induced showers. The efficiency has been computed with Monte Carlo simulations as the fraction of simulated events identified as neutrinos.

In the case of Earth-skimming ν_τ induced showers, and a full Auger SD working without interruption, the efficiencies depend only on the energy of the emerging τ leptons (E_τ) and on the altitude of the "center of the shower" (h_c) above ground (averaged over the decay channels). This is conveniently defined as the altitude of the shower axis at a distance of 10 km away from the τ decay point along the shower axis. Showers induced by τ leptons with the same energy but with different zenith angles—the range in θ being very narrow—have approximately the same efficiency as long as the corresponding altitudes of their shower maxima h_c are the same. The maximum efficiency that can be reached is 82.6%, the 17.4% remaining corresponds to the channel in which the τ decays into a μ which is unlikely to produce a detectable shower close to ground. In Figure 8 we show the trigger and identification efficiencies as a function of h_c for different τ energies. As expected, the efficiency increases with E_τ and drops as the τ decays at increasing altitude from ground.

In the case of downward-going neutrinos the identification efficiency depends on neutrino flavour, type of interaction (CC or NC), neutrino energy (E_ν), zenith angle (θ), and distance (D) measured from ground along the shower

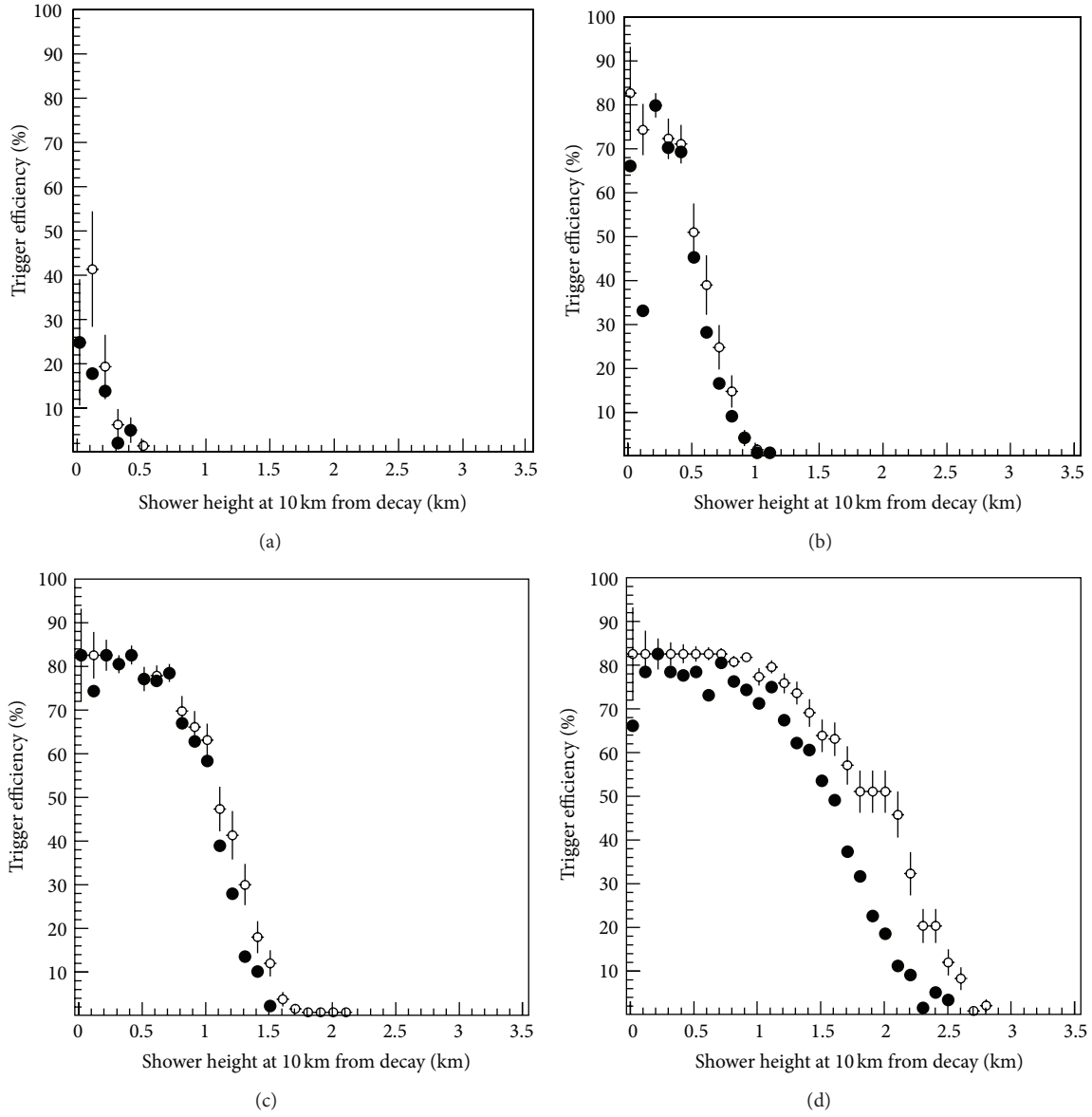

FIGURE 8: T3 trigger (open dots) and identification (closed dots, cuts as in Table 1) efficiency in the Earth-skimming analysis, as a function of the height above ground of the shower at 10 km from the τ decay point h_c. The efficiency is shown for Monte Carlo showers induced by τs with energy (clockwise from (a)) 0.1, 1, 10 and 100 EeV. The efficiencies are calculated in a full SD array (see text for details).

axis at which the neutrino is forced to interact in the simulations. An example of the efficiency that can be achieved in a full SD array is shown in Figure 9. The efficiency is different from zero between a minimal depth close to ground (a minimal amount of matter needed for the ν-induced shower to reach a sufficient lateral expansion), and a maximal one (such that the electromagnetic component is almost extinguished at ground level and hence the neutrino cannot be identified). The efficiency as well as the slice of atmosphere where it is different from zero, typically increase with neutrino energy, and depend on the neutrino flavour and interaction. As an extreme example, high energy ν_τ interacting in the atmosphere through the CC channel can be identified regardless the interaction depth in the atmosphere, as long as the energetic τ produced in the interaction decays and produces a shower close to ground.

6.2. Exposure. Ideally, for the calculation of the exposure of the SD of the Auger Observatory to ultrahigh energy neutrinos, the simulated neutrino showers should be randomly distributed over the actual configurations of the array, applying to the shower at ground the trigger and neutrino identification conditions to obtain the active (effective) area of the array at every second, and as a function of the parameters of the neutrino-induced showers (neutrino energy, zenith angle, h_c, etc.). A sum over time and integration in solid angle would then yield the *exposure* ($\mathscr{E}$) to UHE neutrinos

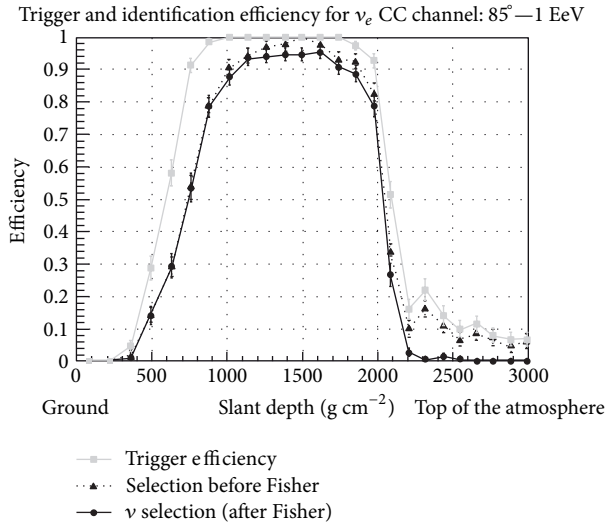

FIGURE 9: Fraction of electron neutrinos of energy 1 EeV and $\theta = 85^\circ$ triggering the array (solid grey line) and passing the downward-going analysis cuts in the second column of Table 1 (solid black line) as a function of the slant depth of the interaction above the ground. The dashed line represents the fraction of events passing all cuts except for the cut on the Fisher discriminant $\mathcal{F}$ (see Section 5.2). The efficiencies are calculated in a full SD array (see text for details).

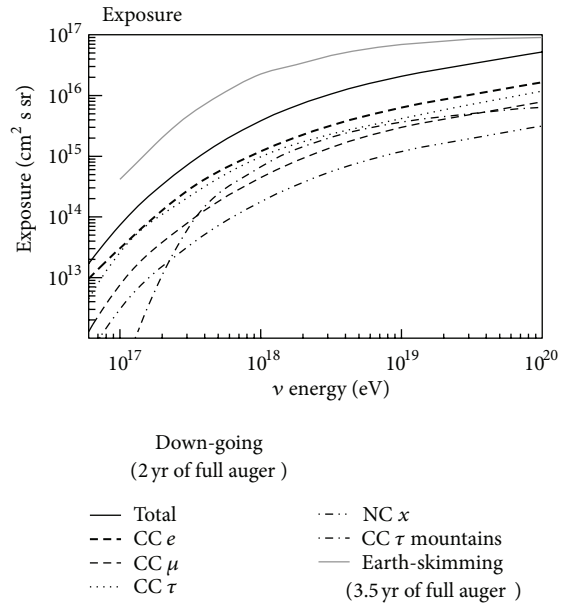

FIGURE 10: Exposure of the surface detector array of the Pierre Auger Observatory on the data search periods to Earth-skimming ν-induced showers (equivalent to 3.5 yr of full Auger) and to downward-going ν-induced showers (equivalent to 2 yr of full Auger).

in both the Earth-skimming and downward-going neutrino analyses. During the search periods considered for both Earth-skimming and downward-going neutrino searches, the surface detector array of the Pierre Auger Observatory was growing continuously. Since the number of working stations and their status are monitored every second, we know with very good accuracy the SD configuration at any instant as well as its evolution with time.

In practice, to avoid having to cope with an unaffordable number of configurations, different strategies were devised to calculate in an accurate and less time-consuming manner the effective area of the SD array to Earth-skimming and downward-going ν-induced showers.

For downward-going neutrinos, the calculation of the exposure involves folding the SD array aperture with the ν interaction probability, the identification efficiency, and integrating in time. Changes in the configuration of the array introduce a dependence of the efficiency ϵ on the position of the core of the shower $\vec{r} = (x, y)$ in the surface S covered by the array and on time t.

Assuming a 1:1:1 flavour ratio (as expected due to the effects of neutrino oscillations during propagation from the sources), the total exposure can be written as [33]:

$$\mathcal{E}^{\mathrm{DG}}(E_\nu) = \frac{2\pi}{m}\sum_i \left[\sigma^i(E_\nu)\int dt\, d\theta\, dD\, \sin\theta\, \cos\theta\, A^i_{\mathrm{eff}}(\theta, D, E_\nu, t)\right], \quad (1)$$

where the sum runs over the three neutrino flavours and the CC and NC interactions, with σ^i the corresponding ν-nucleon interaction cross-section [41] and m the nucleon mass. The integral is performed over the zenith angle θ, the interaction depth D of the neutrino (in units of g cm^{-2}), and the blind search period. A^i_{eff} is the effective area of the SD array given by:

$$A^i_{\mathrm{eff}}(E_\nu, \theta, D, t) = \int \epsilon^i(\vec{r}, \theta, D, E_\nu, t)\, dA, \quad (2)$$

where the integral is performed over the core positions $\vec{r}$ of the showers.

For the Earth-skimming neutrinos the calculation of the exposure is described in [32].

The exposures obtained for the search periods indicated in Table 2 are plotted in Figure 10, where for the downward-going neutrino-induced showers, we also plot the contribution of the different channels (Figure 4) to the total exposure. Among them we have included the possibility that downward-going ν_τs interact with the mountains surrounding the Observatory which provide a dense target for neutrino interactions.

The exposure to Earth-skimming neutrinos is higher than that to downward-going neutrinos by a factor between ~2 and ~7 depending on the neutrino energy, partially due to the longer search period in the Earth-skimming analysis ~3.5 yr of full Auger, compared to ~2.0 yr in the case of the downward-going analysis. When normalized to the same search time, the Earth-skimming channel is still a factor ~2.5–3 more sensitive when integrated over the whole energy range, mainly due to the larger density of the

Table 3: Main sources of systematic uncertainty and their impact on the Earth-skimming [32] and downward-going [33] exposures.

Source of uncertainty	Earth-skimming	Downward-going
Monte Carlo simulation of shower	+20%, −5%	+9%, −33%
ν-nucleon cross-section	+5%, −9%	+7%, −7%
τ energy losses	+25%, −10%	+6%, −6%
Topography	+18%, 0%	—

Earth's crust where ν_τ interactions can occur, compared to the atmosphere. The larger number of neutrino flavours and interaction channels that can be identified in the downward-going analysis, as well as the broader angular range ($75^\circ < \theta < 90^\circ$ compared to $90^\circ < \theta < 95^\circ$), partly compensate the difference.

6.3. Systematic Uncertainties. Several sources of systematic uncertainty have been carefully considered. Some of them are directly related to the Monte Carlo simulation of the showers, that is, generator of the neutrino interaction either in the Earth or in the atmosphere, parton distribution function, air shower development, and hadronic model. Others have to do with the limitations on the theoretical models estimating, for instance, the interaction cross-section or the τ energy loss at high energies. Some of these sources play a dominant role on the Earth-skimming analysis, while others do on the downward-going neutrino one.

In both analyses the procedure to incorporate the systematic uncertainties is the same. Different combinations of the various sources of systematic uncertainty render different values of the exposure, and the final uncertainty is incorporated in the value of the limit itself through a semi-Bayesian extension [42] of the Feldman-Cousins approach [40]. In Table 3 we summarize the dominant sources of systematic uncertainty and their impact on the exposure. In the Earth-skimming analysis the model of energy loss for the τ is the dominant source of uncertainty, since it determines the energy of the emerging τs after propagation in the Earth; the impact of this on the downward-going neutrino analysis is much smaller since τ energy losses are only relevant for ν_τ interacting in the mountains, a channel that is estimated to contribute only ~15% to the total exposure. The uncertainty on the shower simulation, that stems mainly from the different shower propagation codes and hadronic interaction models that can be used to model the high energy collisions in the shower, contributes significantly in both cases. The presence of mountains around the Observatory—which would increase the target for neutrino interactions in both cases—is explicitly simulated and accounted for when obtaining the exposure of the SD to downward-going neutrino-induced showers, and as a consequence does not contribute directly to the systematic uncertainties. However, it is not accounted for in the Earth-skimming limit shown in Table 2. Instead, we take the topography around the observatory as a source of systematic uncertainty and we estimated that accounting for it would have increased the event rate by ~18% (Table 3).

7. Results

We have searched for neutrino candidates over the search data periods and no events fulfilling either the Earth-skimming or the downward-going selection cuts were found. This allows us to put limits to the UHE diffuse neutrino flux.

7.1. Limits to the Diffuse Flux of UHE Neutrinos. Under the assumption that the UHE neutrino flux $\Phi(E)$ behaves with neutrino energy as:

$$\Phi(E) = \frac{dN}{dE} = kE^{-2} \left[\mathrm{GeV}^{-1}\mathrm{cm}^{-2}\mathrm{s}^{-1}\mathrm{sr}^{-1}\right], \quad (3)$$

the *integrated* limit on the value of k is:

$$k = \frac{N_{\mathrm{up}}}{\int_{E_{\mathrm{min}}}^{E_{\mathrm{max}}} E^{-2}\mathscr{E}(E)\,dE}, \quad (4)$$

where $\mathscr{E}(E)$ is the exposure. The actual value of the upper limit on the signal events (N_{up}) depends on the number of observed and expected background events. We recall here that, according to [40], $N_{\mathrm{up}} = 2.44$ at 90% C.L. for zero candidates and no expected background events. When systematic uncertainties are included (Section 6.3) the value of N_{up} changes.

The final limits are reported in Table 2 where we give the normalization k obtained in the search periods (indicated in the same table) for the Earth-skimming and downward-going searches.

In Figure 11 we show the Earth-skimming and downward-going integrated neutrino flux which indicate the level of a diffuse neutrino flux assumed to behave with energy as E^{-2}, needed to detect N_{up} events with a Poisson probability of ~ 90% given the exposure accumulated during the 3.5 years for Earth-skimming neutrinos (2.0 years for downward-going) of equivalent time of a full SD.

Another way of presenting the results is to display the upper limit in differential form. In this procedure we assume that the diffuse neutrino flux behaves as E^{-2} within energy bins of 0.5 width on a decimal logarithmic scale, and is given by $2.44/(0.5\log(10)\cdot E\cdot\mathscr{E}(E))$, assuming again no background. The differential limit obtained in this way is shown in Figure 11 for the Earth-skimming and downward-going cases. We achieve most (~90%) of the sensitivity in the energy range ~0.16–20 EeV (~0.1–100 EeV) for Earth-skimming (downward-going) neutrinos. In Figure 11 we also show several predictions of different theoretical models of

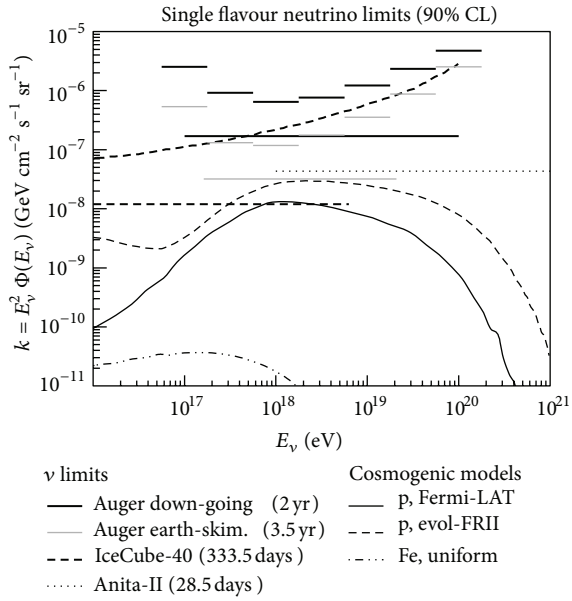

Figure 11: Thick lines represent differential and integrated upper limits (at 90% C.L.) to the diffuse flux of UHE neutrinos (single flavour assuming equipartition) from the Pierre Auger Observatory for downward-going ν (equivalent search period = 2 yr of full Auger) and Earth-skimming ν_τ (equivalent search period = 3.5 yr of full Auger). Limits from other experiments are also plotted [46–48]. All limits have been scaled to single flavour. The IceCube differential limit is scaled by a factor 1/2 due to the different binning in energy with respect to the Auger differential limits. Thin lines: Expected fluxes for three theoretical models of cosmogenic neutrinos (scaled to single flavour when necessary). "p, Fermi-LAT" [43] corresponds to the best fit to UHECR spectrum incorporating the Fermi-LAT bound assuming that the transition from Galactic to extragalactic CRs takes place at 10^{19} eV. "p, evol-FRII" [12] assumes the FRII strong source evolution with a pure proton composition, dip transition model and maximum energy of UHECRs at the sources $E_{p,\max} = 10^{21.5}$ eV. "Fe, uniform" [12] represents an extreme model assuming an iron rich composition, low $E_{p,\max}$, uniform evolution of the UHECR sources.

cosmogenic neutrino production [12, 43]. Predictions for cosmogenic neutrino fluxes depend on several unknown parameters including the evolution with redshift of the sources and the injected UHECR composition. Given the uncertainties in these parameters, and in particular the possible presence of heavy primaries in the UHECR spectrum [49], we have plotted a range of models to illustrate the wide range of predictions available [12].

7.2. Event Rate Predictions. In Table 4 we give the expected number of events from a diffuse flux of cosmogenic neutrinos (produced in the interaction of cosmic ray protons with background radiation fields) [43], from a model of neutrino production through the bottom-up mechanism in Active Galactic Nuclei (AGN) [44], and from a theoretical model [45] in which neutrinos are the product of the decay of superheavy relic particles of the early stages of the Universe. Optimistic theoretical flux predictions for cosmogenic neutrinos are within reach of our present sensitivity and some models of neutrinos produced in accelerating sources are already being constrained. Exotic models are severely disfavored. Note that all such top-down models are also tightly constrained by the limits of the Pierre Auger Observatory on the photon fraction in UHECR [50].

8. Summary and Prospects

In this paper we have reviewed the searches for astrophysical sources of ultrahigh energy neutrinos at the Pierre Auger Observatory [31–33].

The neutrino detection technique is based on the observation of extensive air showers induced by downward-going neutrinos of all flavours as they interact with the atmosphere, and by upward-going ν_τ's through the Earth-skimming mechanism. These ν-induced showers display characteristic features that allow us their identification in the overwhelming background of regular UHE hadronic showers. At ground level, high zenith angle neutrino events would have a significant electromagnetic component leading to a broad time structure of detected signals in the surface detector array, in contrast to nucleonic-induced showers.

We have shown that, using Monte Carlo simulations and training data samples, identification criteria for UHE neutrinos can be defined and used to perform a blind search on the remaining data sample. The analysis of the collected data at the Pierre Auger Observatory until 31 May 2010 reveals no candidate events for either downward-going or Earth-skimming neutrinos. Based on this negative result, stringent limits have been placed on the diffuse flux of UHE neutrinos. Even though the Auger Observatory was designed to measure properties of UHECRs, the limits reported in Table 2 provide at present one of the most sensitive bounds on neutrinos at EeV energies, which is the most relevant energy to explore the predicted fluxes of cosmogenic neutrinos.

There are several lines of work in progress inside the Auger Collaboration related to the neutrino search which will be the subject of future reports. Some of the efforts concentrate on the combination of the downward-going and Earth-skimming channels into a single analysis. This will simplify the search procedure and will obviously translate into an improvement of the diffuse neutrino limit. The extension of the downward-going neutrino search to lower zenith angles ($\theta < 75^\circ$) is also very promising. Exploring the sky down to $\theta \sim 60^\circ$ implies a sizeable increase on the exposure and hence on the limit in case no candidates are found. The main drawback of decreasing θ is that the atmosphere slant depth reduces and nucleonic-induced showers look "younger" when arriving at ground, making their separation from ν-induced showers more challenging. On the other hand, the sensitivity to neutrino detection could also be extended to lower energies by reducing the separation between SD stations. Monte Carlo studies indicate that using a configuration of stations similar to the currently existing "infill" array (~60 stations spaced by 750 m) would lead to a significant increase of the neutrino detection probability at lower energies (below 0.3 EeV) with respect to the standard

Table 4: Number of expected events for several theoretical models of UHE neutrino production, given the exposure of the surface detector array of the Pierre Auger Observatory to earth-skimming and downward-going neutrinos (Table 2).

Model and reference	Earth-skimming	Downward-going
Cosmogenic (Fermi) [43]	~0.6	~0.1
AGN [44]	~5.1	~0.8
Exotic (SH relics) [45]	~3.0	~1.0

SD array. Nevertheless, due to the small size of the current infill array, the exposure does not appear to be competitive.

Finally, it is worth mentioning that the sensitivity of the Pierre Auger Observatory to the detection of UHEνs from potential astrophysical *point-like* sources is being evaluated. The absence of candidates in the searches for diffuse neutrino fluxes described in this report allows us to place limits on the neutrino fluxes coming from sources in the field of view of the SD of the Auger Observatory. Preliminary results indicate that with the SD we are sensitive to a large fraction of the sky spanning ~100° in declination [51].

Acknowledgments

The successful installation, commissioning, and operation of the Pierre Auger Observatory would not have been possible without the strong commitment and effort from the technical and administrative staff in Malargüe. The authors are very grateful to the following agencies and organizations for financial support: Comisión Nacional de Energía Atómica, Fundación Antorchas, Gobierno De La Provincia de Mendoza, Municipalidad de Malargüe, NDM Holdings and Valle Las Leñas, in gratitude for their continuing cooperation over land access, Argentina; the Australian Research Council; Conselho Nacional de Desenvolvimento Científico e Tecnológico (CNPq), Financiadora de Estudos e Projetos (FINEP), Fundação de Amparo à Pesquisa do Estado de Rio de Janeiro (FAPERJ), Fundação de Amparo à Pesquisa do Estado de São Paulo (FAPESP), Ministério de Ciência e Tecnologia (MCT), Brazil; AVCR AV0Z10100502 and AV0Z10100522, GAAV KJB100100904, MSMT-CR LA08016, LG11044, MEB111003, MSM0021620859, LA08015, and TACR TA01010517, Czech Republic; Centre de Calcul IN2P3/CNRS, Centre National de la Recherche Scientifique (CNRS), Conseil Régional Ile-de-France, Département Physique Nucléaire et Corpusculaire (PNC-IN2P3/CNRS), Département Sciences de l'Univers (SDU-INSU/CNRS), France; Bundesministerium für Bildung und Forschung (BMBF), Deutsche Forschungsgemeinschaft (DFG), Finanzministerium Baden-Württemberg, Helmholtz-Gemeinschaft Deutscher Forschungszentren (HGF), Ministerium für Wissenschaft und Forschung, Nordrhein-Westfalen, Ministerium für Wissenschaft, Forschung und Kunst, Baden-Württemberg, Germany; Istituto Nazionale di Fisica Nucleare (INFN), Ministero dell'Istruzione, dell'Università e della Ricerca (MIUR), Italy; Consejo Nacional de Ciencia y Tecnología (CONACYT), Mexico; Ministerie van Onderwijs, Cultuur en Wetenschap, Nederlandse Organisatie voor Wetenschappelijk Onderzoek (NWO), Stichting voor Fundamenteel Onderzoek der Materie (FOM), The Netherlands; Ministry of Science and Higher Education, Grants no. N N202 200239 and N N202 2038, Poland; Fundação para a Ciência e a Tecnologia, Portugal; Ministry for Higher Education, Science, and Technology, Slovenian Research Agency, Slovenia; Comunidad de Madrid, Consejería de Educación de la Comunidad de Castilla La Mancha, FEDER funds, Ministerio de Ciencia e Innovación and Consolider-Ingenio 2010 (CPAN), Xunta de Galicia, Spain; Science and Technology Facilities Council, UK; Department of Energy, Contract nos. DE-AC02-07CH11359 and DE-FR02-04ER41300, National Science Foundation, Grant no. 0450696, The Grainger Foundation, USA; NAFOSTED, Vietnam; ALFA-EC/HELEN and UNESCO.

References

[1] M. Nagano and A. A. Watson, "Observations and implications of the ultrahigh-energy cosmic rays," *Reviews of Modern Physics*, vol. 72, no. 3, pp. 689–732, 2000.

[2] K. Kotera and A. Olinto, "The astrophysics of ultrahigh-energy cosmic rays," *Annual Review of Astronomy and Astrophysics*, vol. 49, pp. 119–153, 2010.

[3] F. Halzen and D. Hooper, "High-energy neutrino astronomy: the cosmic ray connection," *Reports on Progress in Physics*, vol. 65, no. 7, p. 1025, 2002.

[4] J. K. Becker, "High-energy neutrinos in the context of multi-messenger astrophysics," *Physics Reports*, vol. 458, no. 4-5, pp. 173–246, 2008.

[5] P. Bhattacharjee and G. Sigl, "Origin and propagation of extremely high-energy cosmic rays," *Physics Reports*, vol. 327, no. 3-4, pp. 109–247, 2000.

[6] K. Greisen, "End to the cosmic-ray spectrum?" *Physical Review Letters*, vol. 16, pp. 748–750, 1966.

[7] G. T. Zatsepin and V. A. Kuzmin, "Upper limit of the spectrum of cosmic rays," *Pis'ma v Zhurnal Eksperimental noi i Teoretich-eskoi Fiziki*, vol. 4, p. 114, 1966, English translation in: *JETP Letters*, vol. 4, p. 78, 1966.

[8] V. S. Berezinsky and G. T. Zatsepin, "Cosmic rays at ultra high energies (neutrino?)," *Physics Letters B*, vol. 28, no. 6, pp. 423–424, 1969.

[9] R. U. Abbasi, T. Abu-Zayyad, M. Allen et al., "First Observation of the Greisen-Zatsepin-Kuzmin Suppression," *Physical Review Letters*, vol. 100, no. 10, article 101101, 5 pages, 2008.

[10] J. Abraham, P. Abreu, M. Aglietta et al., "Observation of the suppression of the flux of cosmic rays above 4×10^{19} eV," *Physical Review Letters*, vol. 101, no. 6, article 061101, 7 pages, 2008.

[11] J. Abraham, P. Abreu, M. Aglietta et al., "Measurement of the energy spectrum of cosmic rays above 10^{18} eV using the pierre auger observatory," *Physical Letters B*, vol. 685, no. 4-5, pp. 239–246, 2010.

[12] K. Kotera, D. Allard, and A. V. Olinto, "Cosmogenic neutrinos: parameter space and detectabilty from PeV to ZeV," *Journal of Cosmology and Astroparticle Physics*, vol. 2010, no. 10, article 013, 2010.

[13] D. Seckel and T. Stanev, "Neutrinos: the key to ultrahigh energy cosmic rays," *Physical Review Letters*, vol. 95, no. 14, article 141101, 3 pages, 2005.

[14] D. Allard, M. Ave, N. Busca et al., "Cosmogenic Neutrinos from the propagation of Ultra High Energy Nuclei," *Journal of Cosmology and Astroparticle Physics*, vol. 2006, no. 09, article 005, 2006.

[15] B. Baret and V. van Elewyck, "High-energy neutrino astronomy: detection methods and first achievements," *Reports on Progress in Physics*, vol. 74, no. 4, article 046902, 2011.

[16] L. A. Anchordoqui and T. Montaruli, "In search of extraterrestrial high-energy neutrinos," *Annual Review of Nuclear and Particle Science*, vol. 60, pp. 129–162, 2010.

[17] E. Zas, "Neutrino detection with inclined air showers," *New Journal of Physics*, vol. 7, p. 130, 2005.

[18] V. S. Berezinsky and A. Yu. Smirnov, "Cosmic neutrinos of ultrahigh energies and detection possibility," *Astrophysics and Space Science*, vol. 32, no. 2, pp. 461–482, 1975.

[19] T. Hara et al., "Observation of air showers of energies above 10^{18}eV," *Acta physica Academiae Scientiarum Hungaricae*, vol. 29, supplement 3, p. 361, 1970, Proceedings of the 11th International Conference on Cosmic Rays (Budapest).

[20] M. Nagano, T. Hara, S. Kawaguchi et al., "Horizontal air showers of energies above 10^{13} eV," *Journal of the Physical Society of Japan*, vol. 30, pp. 33–55, 1971.

[21] A. M. Hillas et al., "Calculations of the particle and energy loss densities in extensive air showers at large radial distances," *Acta Physica Academiae Scientarum Hungaricae*, vol. 29, supplement 3, p. 533, 1970, Proceedings of the 11th International Conference on Cosmic Rays (Budapest).

[22] D. Andrews, A. C. Evans, R. R. Hughes et al., "General results from the Haverah Park large E. A. S. array," *Acta Physica Academiae Scientarum Hungaricae*, vol. 29, p. 337, 1970.

[23] J. Abraham, M. Aglietta, I. C. Aguirre et al., "Properties and performance of the prototype instrument for the Pierre Auger Observatory," *Nuclear Instruments and Methods in Physics Research A*, vol. 523, no. 1-2, pp. 50–95, 2004.

[24] K. S. Capelle, J. W. Cronin, G. Parente, and E. Zas, "On the detection of ultra high energy neutrinos with the Auger observatory," *Astroparticle Physics*, vol. 8, no. 4, pp. 321–328, 1998.

[25] P. Billoir et al., "The pierre auger observatory and neutrinos," in *Proceedings of the Neutrino Oscillation Workshop (NOW '06)*, Lecce, Italy, 2006.

[26] X. Bertou, P. Billoir, O. Deligny, C. Lachaud, and A. Letessier-Selvon, "Tau neutrinos in the Auger Observatory: a new window to UHECR sources," *Astroparticle Physics*, vol. 17, no. 2, pp. 183–193, 2002.

[27] D. Fargion, "Discovering ultra-high-energy neutrinos through horizontal and upward τ air showers: evidence in terrestrial gamma flashes? " *The Astrophysical Journal*, vol. 570, no. 2, pp. 909–925, 2002.

[28] I. Allekotte et al., "The surface detector system of the Pierre Auger Observatory," *Nuclear Instruments and Methods in Physics Research A*, vol. 586, no. 3, pp. 409–420, 2008.

[29] X. Bertou, P. S. Allison, C. Bonifazi et al., "Calibration of the surface array of the Pierre Auger Observatory," *Nuclear Instruments and Methods in Physics Research A*, vol. 568, no. 2, pp. 839–846, 2006.

[30] J. Abraham, P. Abreu, M. Aglietta et al., "Trigger and aperture of the surface detector array of the Pierre Auger Observatory," *Nuclear Instruments and Methods in Physics Research A*, vol. 613, no. 1, pp. 29–39, 2010.

[31] J. Abraham, P. Abreu, M. Aglietta et al., "Upper limit on the diffuse flux of ultrahigh energy tau neutrinos from the Pierre Auger Observatory," *Physical Review Letters*, vol. 100, no. 21, article 211101, Article ID 211101, 2008.

[32] J. Abraham, P. Abreu, M. Aglietta et al., "Limit on the diffuse flux of ultrahigh energy tau neutrinos with the surface detector of the Pierre Auger Observatory," *Physical Review D*, vol. 79, no. 10, article 211101, 2009.

[33] P. Abreu, M. Aglietta, E. J. Ahn et al., "Search for ultrahigh energy neutrinos in highly inclined events at the Pierre Auger Observatory," *Physical Review D*, vol. 84, no. 12, article 122005, 2011.

[34] G. Corcella, I. G. Knowles, G. Marchesini et al., "HERWIG 6: an event generator for hadron emission reactions with interfering gluons (including supersymmetric processes)," *Journal of High Energy Physics*, vol. 2001, no. 01, article 010, 2001.

[35] S. Jadach and Z. Was, "The τ decay library TAUOLA, version 2.4," *Computer Physics Communications*, vol. 76, no. 3, pp. 361–380, 1993.

[36] S. J. Sciutto, arXiv:astro-ph/9911331, http://www2.fisica.unlp.edu.ar/auger/aires/ppal.html.

[37] S. Argiró, S. Barroso, J. Gonzalez et al., "The offline software framework of the Pierre Auger Observatory," *Nuclear Instruments and Methods in Physics Research A*, vol. 580, no. 3, pp. 1485–1496, 2007.

[38] http://geant4.web.cern.ch/geant4/.

[39] R. Fisher, "The use of multiple measurements in taxonomic problems," *Annals of Eugenics*, vol. 7, no. 2, pp. 179–188, 1936.

[40] G. J. Feldman and R. D. Cousins, "Unified approach to the classical statistical analysis of small signals," *Physical Review D*, vol. 57, no. 7, pp. 3873–3889, 1998.

[41] A. Cooper-Sarkar and S. Sarkar, "Predictions for high energy neutrino cross-sections from the ZEUS global PDF fits," *Journal of High Energy Physics*, vol. 01, article 075, 2008.

[42] J. Conrad et al., "Including systematic uncertainties in confidence interval construction for Poisson statistics," *Physical Review D*, vol. 67, no. 1, article 012002, 11 pages, 2003.

[43] M. Ahlers, L. A. Anchordoqui, M. C. Gonzalez-Garcia, F. Halzen, and S. Sarkar, "GZK neutrinos after the Fermi-LAT diffuse photon flux measurement," *Astroparticle Physics*, vol. 34, no. 2, pp. 106–115, 2010.

[44] J. K. Becker, P. L. Biermann, and W. Rhode, "The diffuse neutrino flux from FR-II radio galaxies and blazars: a source property based estimate," *Astroparticle Physics*, vol. 23, no. 4, pp. 355–368, 2005.

[45] O. Kalashev, V. A. Kuzmin, D. V. Semikoz, and G. Sigl, "Ultrahigh-energy neutrino fluxes and their constraints," *Physical Review D*, vol. 66, article 063004, 11 pages, 2002.

[46] R. Abbasi, Y. Abdou, T. Abu-Zayyad et al., "Constraints on the extremely-high energy cosmic neutrino flux with the IceCube 2008-2009 data," *Physical Review D*, vol. 83, no. 9, article 092003, 2011.

[47] P. W. Gorham, P. Allison, S. W. Barwick et al., "New limits on the ultrahigh energy cosmic neutrino flux from the ANITA experiment," *Physical Review Letters*, vol. 103, article 051103, 5 pages, 2009.

[48] P. W. Gorham, P. Allison, S. W. Barwick et al., "The antarctic impulsive transient antenna ultra-high energy neutrino detector: design, performance, and sensitivity for the 2006-2007 balloon flight," *Astroparticle Physics*, vol. 32, no. 1, pp. 10–41, 2009.

[49] P. Abreu, J. Abraham, M. Aglietta et al., "Measurement of the depth of maximum of extensive air showers above 10^{18} eV," *Physical Review Letters*, vol. 104, no. 9, article 091101, 2010.

[50] J. Abraham, P. Abreu, M. Aglietta et al., "Upper limit on the cosmic-ray photon fraction at EeV energies from the Pierre Auger Observatory," *Astroparticle Physics*, vol. 31, no. 6, pp. 399–406, 2009.

[51] P. Abreu, M. Aglietta, M. Ahlers et al., "Search for point-like sources of ultra-high energy neutrinos at the Pierre Auger Observatory and improved limit on the diffuse flux of tau neutrinos," *Astrophysical Journal Letters*, vol. 755, p. L4, 2012.